INTERNATIONAL JOURNAL FOR NUMERICAL METHODS IN FLUIDS, VOL. 25, 907–929 (1997)

A BOUNDARY ELEMENT METHOD FOR STEADY VISCOUS FLUID FLOW USING PENALTY FUNCTION FORMULATION

M. M. GRIGORIEV* AND A. V. FAFURIN

Kazan State Technology University, K. Marx Street 68, Kazan 420015, Russia

SUMMARY

A new boundary element method is presented for steady incompressible flow at moderate and high Reynolds numbers. The whole domain is discretized into a number of eight-noded cells, for each of which the governing boundary integral equation is formulated exclusively in terms of velocities and tractions. The kernels used in this paper are the fundamental solutions of the linearized Navier–Stokes equations with artificial compressibility. Significant attention is given to the numerical evaluation of the integrals over quadratic boundary elements as well as over quadratic quadrilateral volume cells in order to ensure a high accuracy level at high Reynolds numbers. As an illustration, square driven cavity flows are considered for Reynolds numbers up to 1000. Numerical results demonstrate both the high convergence rate, even when using simple (direct) iterations, and the appropriate level of accuracy of the proposed method. Although the method yields a high level of accuracy in the primary vortex region, the secondary vortices are not properly resolved. © 1997 John Wiley & Sons, Ltd.

Int. J. Numer. Meth. Fluids, **25**: 907–929 (1997)

No. of Figures: 5. No. of Tables: 1. No. of References: 26.

KEY WORDS: Navier–Stokes equations; penalty function formulation; boundary element method; driven cavity flow

1. INTRODUCTION

Searches for novel numerical approaches different from finite difference and finite element techniques have led to a rapid progress of boundary element methods for the past decade. However, boundary element methods can conventionally be referred to as 'novel' only, because these numerical methods have roots stretching back to the pioneering works of Oseen,[1] Muskhelishvili,[2] Mikhlin[3] and Ladyzhenskaya[4] and are closely related to boundary integral equation methods. Having evolved since the early 1980s, several monographs[5–7] and an abundance of papers devoted to boundary element techniques are indicative of growing interest in these numerical methods.

By now a large number of boundary element formulations have been implemented fully utilizing the advantages over other numerical approaches, among which the unity decreasing should be highlighted; that is, only the boundary of the domain is to be discretized. It is well known that boundary value problems may be represented in terms of boundary integral equations involving the boundary unknowns and their derivatives solely for problems governed by linear differential

* Correspondence to: M. M. Grigoriev, Kazan State Technology University, K. Marx Street 68, Kazan 420015, Russia.

Contract grant sponsor: Russian Fund of Basic Research; Contract grant number: 96-02-16751-a.

CCC 0271–2091/97/080907–23 $17.50

Received March 1996
Revised November 1996

equations. Unfortunately, viscous fluid flow is governed by the non-linear Navier–Stokes equations and hence a boundary value problem cannot be reduced to a boundary integral equation only and the advantages of boundary element methods are offset. One is forced to accept the fact that the boundary element techniques for viscous fluid dynamics proposed to date are considerably inferior to the most sophisticated finite element methods in terms of efficiency. When numerically modelling viscous fluid flow, the non-linear convective term has most often been considered as a pseudo-body force; this being so, the linear differential equation remaining might be easily converted to boundary integral form. In that instance, fundamental solutions are utilized which do not take into consideration the convective nature of the flow. Specifically, Onishi *et al.*,[8] Skerget *et al.*,[9] Camp and Gipson,[10] Wu[11] and Grigor'ev[12] used fundamental solutions of the Laplace equation, Tosaka *et al.*[13] and Dargush and Banerjee[14] utilized fundamental solutions of Stokes flow, while Kitagawa *et al.*[15] and Kitagawa[16] used fundamental solutions of the Navier equation. We emphasize that this approach allows one to calculate velocities at the boundary and internal nodes separately, yet such a nodal value splitting permits one to use only simple iterations in order to solve the set of non-linear equations. Built upon this approach, numerical techniques were stable only at low Reynolds numbers. Attempts to improve the numerical method by utilizing a Newton–Raphson algorithm necessitated a simultaneous consideration of every boundary and internal nodal value and resulted in a densely populated square matrix of great size. Evidently, in actual practice, these numerical approaches, especially for a large number of nodal variables, have failed.

It is reasonably safe to suggest that one way of developing a high-performance boundary element method is to employ kernel functions taking into account the convective nature of the flow. In particular, the harnessing of the half-forgotten Oseen fundamental solutions, which were undeservedly relegated to the background with the advent of digital computers and the rapid progression of numerical methods, holds much promise. It should be noted that numerical methods, like finite difference and finite element methods as well as spectral methods, are incapable of incorporating any solution of Oseen's kind. Only at the specific stage of boundary element technique advancement do we have considerable opportunity to revert to the classical Oseen solutions.[1]

It must be emphasized that there were few attempts[17,18] to utilize these fundamental solutions with linearized convective terms. Unfortunately, the behaviour of the convective kernel function was not properly considered and hence the proposed methods were not accurate even at moderate Reynolds numbers. Moreover, Kakuda and Tosaka[17] reported that the Newton–Raphson algorithm was required to obtain convergent solutions. It is evident that in order to develop a highly efficient boundary element method utilizing Oseenlets, coefficients of boundary integral equations should be evaluated to high accuracy especially at high Reynolds numbers.

In this paper a new boundary element method is presented for numerical modelling of the Navier–Stokes equations. The kernels used here are the fundamental solutions of the linearized Navier–Stokes equations with artificial compressibility. The utilization of weighting functions incorporating convective velocities and the linearization of the Navier–Stokes equations within the subdomains make it possible to implement the efficient numerical method for steady viscous fluid flow modelling up to high Reynolds numbers.

2. GOVERNING EQUATIONS AND FUNDAMENTAL SOLUTIONS

Steady state viscous fluid flow is governed by the continuity equation

$$\frac{\partial u_i}{\partial x_i} = 0, \tag{1}$$

which expresses the conservation law of mass, and the Navier–Stokes equation

$$u_j \frac{\partial u_i}{\partial x_j} = -\frac{\partial p}{\partial x_i} + v \frac{\partial}{\partial x_j}\left(\frac{\partial u_j}{\partial x_i} + \frac{\partial u_i}{\partial x_j}\right), \tag{2}$$

which expresses the conservation law of momentum. In the dimensionless equations (1) and (2), x_i is the Eulerian co-ordinate, u_i is the flow velocity, p is the pressure and v is the viscosity.

Let us consider a penalty function formulation which implies an artificial compressibility of the flow,

$$p = -\lambda \frac{\partial u_i}{\partial x_i}, \tag{3}$$

where the penalty parameter λ is chosen large enough ($\lambda > 10^5$) to attain low values of velocity dilatation. The set of equations will have a unique solution if the boundary conditions are properly specified as

$$\bar{u}_i \quad \text{on } \Gamma_1, \qquad \bar{t}_i \quad \text{on } \Gamma_2, \tag{4}$$

where Γ_1 and Γ_2 are subregions of Γ satisfying $\Gamma_1 \cup \Gamma_2 = \Gamma$ and $\Gamma_1 \cap \Gamma_2 = \oslash$, while Γ is the complete surface bounding the domain Ω.

The momentum equation (2) may be linearized through the discretization of the whole domain Ω into N_c subdomains Ω_n, where $n = 1, 2, \ldots, N_c$, and through the decomposition of the convective velocity into the sum

$$u_i = V_i^{(n)} + u_i' \tag{5}$$

for each subdomain. In (5), $V_i^{(n)}$ is the specific constant velocity of the flow in subdomain Ω_n and its value may be taken to be equal to the averaged velocity over the subdomain,

$$V_i^{(n)} = \int_{\Omega_n} u_i \, d\Omega \Big/ \int_{\Omega_n} d\Omega.$$

Substituting (3) and (5) into (2), we have

$$V_j^{(n)} \frac{\partial u_i}{\partial x_j} + u_j' \frac{\partial u_i}{\partial x_j} = \frac{\partial \sigma_{ij}}{\partial x_j}, \tag{6}$$

in which the stress tensor may be represented in the form

$$\sigma_{ij} = 2v\varepsilon_{ij} + \lambda \varepsilon_{mm} \delta_{ij}.$$

In the last equation, δ_{ij} is the Kronecker delta and

$$\varepsilon_{ij} = \frac{1}{2}\left(\frac{\partial u_i}{\partial x_j} + \frac{\partial u_j}{\partial x_i}\right)$$

is the rate-of-deformation tensor. Equation (6) will be linear if the velocity perturbation u_j' is assumed to be equal to zero over the subdomain. In this instance we are concerned with the linearization of the Navier–Stokes equations provided by Oseen:

$$V_j^{(n)} \frac{\partial u_i}{\partial x_j} = \frac{\partial \sigma_{ij}}{\partial x_j}. \tag{7}$$

Hereafter we shall omit index n for brevity, implying each subdomain Ω_n. Oseen, in his classical monograph,[1] derived fundamental solutions of incompressible flow governed by the linearized Navier–Stokes equation

$$V_j \frac{\partial u_i}{\partial x_j} = -\frac{\partial p}{\partial x_i} + \nu \frac{\partial^2 u_i}{\partial x_j \partial x_j}. \tag{8}$$

These solutions may be written as*

$$u^*_{ik}(V, y) = \frac{1}{4\pi\nu}\left\{\delta_{ik}\exp\left(-\frac{y_j V_j}{2\nu}\right)K_0\left(\frac{rV}{2\nu}\right) + \frac{1}{rV}(y_i V_k + y_k V_i - \delta_{ik} y_j V_j)\left[\frac{2\nu}{rV} - \exp\left(-\frac{y_j V_j}{2\nu}\right)K_1\left(\frac{rV}{2\nu}\right)\right]\right\}, \tag{9a}$$

$$q_k = -\frac{y_k}{2\pi r^2}. \tag{9b}$$

In (9a,b) we define

$$y_i = x_i - \xi_i, \qquad r^2 = y_i y_i, \qquad V^2 = V_i V_i,$$

$K_0(.)$ and $K_1(.)$ are modified Bessel functions of the second kind of zeroth and first order respectively, x_i is the field point and ξ_i is the source point. Functions (9a,b) constitute nothing but the solution of the set of equations

$$V_j \frac{\partial u^*_{ik}}{\partial x_j} + \nu \frac{\partial^2 u^*_{ik}}{\partial x_j \partial x_j} + \frac{\partial q_k}{\partial x_i} + \delta_{ik}\delta(x - \xi) = 0, \tag{10}$$

$$\frac{\partial u^*_{ik}}{\partial x_i} = 0 \tag{11}$$

for infinite unbounded plane flow with constant convective velocity V_i. In (10), $\delta(x - \xi)$ is the Dirac delta function. Functions (9) incorporating the convective flow velocity are fully suited for numerical implementation of the efficient boundary element method, but the surprising thing is that the Oseen solutions (9) have not been implemented in full measure to demonstrate their capabilities!

When using the penalty function formulation, we can derive fundamental solutions of (7) as

$$u^*_{ik}(V, y) = \frac{1}{4\pi\nu}\left\{\delta_{ik}\exp\left(-\frac{y_j V_j}{2\nu}\right)K_0\left(\frac{rV}{2\nu}\right) + \frac{1}{rV}(V_i y_k + V_k y_i - \delta_{ik} y_j V_j) \times \left[\frac{2\nu}{rV} - \exp\left(-\frac{y_j V_j}{2\nu}\right)K_1\left(\frac{rV}{2\nu}\right)\right]\right\} - \frac{1}{4\pi\mu}\left\{-\delta_{ik}\exp\left(-\frac{y_j V_j}{2\mu}\right)K_0\left(\frac{rV}{2\mu}\right) + \frac{1}{rV}(V_i y_k + V_k y_i - \delta_{ik} y_j V_j)\left[\frac{2\mu}{rV} - \exp\left(-\frac{y_j V_j}{2\mu}\right)K_1\left(\frac{rV}{2\mu}\right)\right]\right\}, \tag{12}$$

which satisfy the equation

$$V_j \frac{\partial u^*_{ik}}{\partial x_j} + \frac{\partial \sigma^*_{ijk}}{\partial x_j} + \delta_{ik}\delta(x - \xi) = 0. \tag{13}$$

* The Oseen solutions written in this form were provided by Dr. G. F. Dargush, State University of New York at Buffalo, to the first author and we gratefully acknowledge this contribution.

In (12) and (13) the notation

$$\sigma^*_{ijk} = 2v\varepsilon^*_{ijk} + \lambda\varepsilon^*_{mmk}\delta_{ij}, \qquad \varepsilon^*_{ijk} = \frac{1}{2}\left(\frac{\partial u^*_{ik}}{\partial x_j} + \frac{\partial u^*_{jk}}{\partial x_i}\right), \qquad \mu = \lambda + 2v$$

is introduced. Now that we have presented the fundamental solution of the Navier–Stokes equation with artificial compressibility, let us examine its distinguishing features. We draw attention to the fact that solution (12) transforms to the Oseen fundamental solution (9) at $1/\lambda = 0$. Furthermore, if the convective velocity is virtually zero, solution (12) reduces to the well-known Kelvin fundamental solution[6,16]

$$u^*_{ik} = \frac{1}{4\pi v}\left[\left(1 - \frac{v}{\mu}\right)\frac{y_i y_k}{r^2} - \left(1 + \frac{v}{\mu}\right)\delta_{ik}\ln r\right] \tag{14}$$

of the Navier equation

$$v\frac{\partial^2 u_i}{\partial x_j \partial x_j} + (\lambda + v)\frac{\partial^2 u_j}{\partial x_i x_j} = 0.$$

When the convective velocity is equal to zero and the compressibility parameter tends to infinity, expression (12) converts to the Stokeslet

$$u^*_{ik} = \frac{1}{4\pi v}\left(\frac{y_i y_k}{r^2} - \delta_{ik}\ln r\right) \tag{15}$$

satisfying the Stokes equation

$$v\frac{\partial^2 u_i}{\partial x_j \partial x_j} = -\frac{\partial p}{\partial x_i}, \qquad \frac{\partial u_i}{\partial x_i} = 0.$$

Moreover, function (12) tends to zero as one travels from the source node, i.e. as the radius r approaches infinity. Conversely, u^*_{ik} tends to infinity as $r \to 0$. The tensor u^*_{ik} is symmetric, i.e. $u^*_{12} = u^*_{21}$. What is more, it is easy to verify that $u^*_{11} = -u^*_{22}$. As may be seen, the fundamental solutions change dramatically, especially at high Reynolds numbers. Because of this, particular emphasis should be placed on the numerical evaluation of integrals over boundary elements involving the source node.

3. BOUNDARY INTEGRAL EQUATION

Let us consider the tensors

$$T^*_{jk} = u_i\sigma^*_{ijk}, \qquad T_{jk} = \sigma_{ij}u^*_{ik}.$$

Then, using the identities[19]

$$\int_\Omega \left(\frac{\partial T_{jk}}{\partial x_j} - \frac{\partial T^*_{jk}}{\partial x_j}\right) \mathrm{d}\Omega = \int_\Gamma (T_{jk} - T^*_{jk})n_j \,\mathrm{d}\Gamma, \qquad \sigma_{ij}\frac{\partial u^*_{ik}}{\partial x_j} = \frac{\partial u_i}{\partial x_j}\sigma^*_{ijk},$$

we transform equation (6) to the boundary integral equation

$$c_{ik}(\xi)u_i(\xi) + \int_\Gamma u_i(x)t^*_{ik}(V,y)\,\mathrm{d}\Gamma(x) + \int_\Gamma u_i(x)u_j(x)n_j(x)u^*_{ik}(V,y)\,\mathrm{d}\Gamma(x) = \int_\Gamma t_i(x)u^*_{ik}(V,y)\,\mathrm{d}\Gamma(x) + \int_\Omega u_i(x)u'_j(x)\frac{\partial u^*_{ik}(V,y)}{\partial x_j}\mathrm{d}\Omega(x). \tag{16}$$

In the boundary integral equation (16), $t_i(x) = \sigma_{ij}(x)n_j(x)$ is the traction, $n_i(x)$ is the local unit outward normal to the surface Γ and $t^*_{ik}(V,y) = \sigma^*_{ijk}(V,y)n_j$ is the stress tensor associated with the Green function (12). The coefficient $c_{ik}(\xi)$ depends upon the location of the source point. When the point ξ is inside Ω, $c_{ik}(\xi) = \delta_{ik}$. If the source node is outside the domain Ω, $c_{ik}(\xi) = 0$. For ξ located right on the smooth boundary Γ, the coefficient $c_{ij}(\xi)$ is equal to $\frac{1}{2}\delta_{ik}$. In the general case the collocation node ξ may be situated at the corners where the unit normal n_i is subject to a discontinuity and, in consequence, the value of $c_{ik}(\xi)$ is determined by the relative smoothness of the boundary Γ at ξ. However, as indicated later, the values of $c_{ik}(\xi)$ need not be evaluated in an explicit form, since this coefficient will be found in an indirect manner coincidentally with the evaluation of coefficients of the discretized boundary integral equation.

We draw attention to the fact that the boundary integral equation (16) contains no velocity derivatives, thus eliminating the need for their evaluation.

4. NUMERICAL IMPLEMENTATION

4.1. Spatial discretization

Consider an eight-noded cell for the geometric representation of the subdomain Ω_n, for which biquadratic shape functions are introduced to approximate the geometric and functional variation within the volume cell:

$$\varphi = \sum_{\alpha=1}^{8} \varphi^{(\alpha)} M_\alpha(\eta_1, \eta_2). \tag{17}$$

In (17), $\varphi^{(\alpha)}$ represent the nodal values of x_i, u_i and t_i, the shape functions are defined as usual (see Reference 5 for details), while η_1 and η_2 are the intrinsic co-ordinates of the volume cell. Once the cell is introduced, four boundary elements are automatically defined, in which quadratic shape functions are specified:[5]

$$\varphi = \sum_{\alpha=1}^{3} \varphi^{(\alpha)} N_\alpha(\eta). \tag{18}$$

Discretizing the integral equation (16) using quadratic boundary elements and biquadratic volume cells, we obtain

$$c_m u_{km} + \sum_{n=1}^{4}\sum_{\alpha=1}^{3}\sum_{i=1}^{2} u^{(\alpha)}_{in} G^{(\alpha)}_{ikmn} + \sum_{n=1}^{4}\sum_{\alpha=1}^{3}\sum_{i=1}^{2} u^{(\alpha)}_{in} F^{(\alpha)}_{ikmn} = \sum_{n=1}^{4}\sum_{\alpha=1}^{3}\sum_{i=1}^{2} t^{(\alpha)}_{in} H^{(\alpha)}_{ikmn} + \sum_{\alpha=1}^{8}\sum_{i=1}^{2} u^{(\alpha)}_i \hat{V}^{(\alpha)}_{ikm}, \tag{19}$$

where

$$G^{(\alpha)}_{ikmn} = \int_{\Gamma_n} N_\alpha(\eta) t^*_{ik}(V, y^{(m)})\, \mathrm{d}\Gamma(x), \tag{20a}$$

$$H^{(\alpha)}_{ikmn} = \int_{\Gamma_n} N_\alpha(\eta) u^*_{ik}(V, y^{(m)})\, \mathrm{d}\Gamma(x), \tag{20b}$$

$$\tilde{F}^{(\alpha,\beta)}_{ikmn} = \int_{\Gamma_n} N_\alpha(\eta) N_\beta(\eta) u^*_{ik}(V, y^{(m)})\, \mathrm{d}\Gamma(x), \tag{20c}$$

$$F^{(\alpha)}_{ikmn} = \sum_{\beta=1}^{3} \sum_{j=1}^{2} u_j^{(\beta)} n_j \tilde{F}^{(\alpha,\beta)}_{ikmn},$$

$$\tilde{V}^{(\alpha,\beta)}_{ijkm} = \int_{\Omega} M_\alpha(\eta_1, \eta_2) M_\beta(\eta_1, \eta_2) \frac{\partial u^*_{ik}(V, y^{(m)})}{\partial x_j}\, \mathrm{d}\Omega(x), \tag{20d}$$

$$\hat{V}^{(\alpha)}_{ikm} = \sum_{\beta=1}^{8} \sum_{j=1}^{2} u_j'^{(\beta)} \tilde{V}^{(\alpha,\beta)}_{ijkm}.$$

As mentioned above, the fundamental solution (12) exhibits a complex nature upon approaching infinity from the source node. It is apparent that the validity of the presented boundary element method depends mainly on the accuracy of obtaining integrals (20). When integrating over a boundary element Γ_n, we distinguish three categories of singularity:

(i) non-singular case, when the collocation node is located far from the boundary element, i.e. $h \geqslant h_q$
(ii) quasi-singular case, when the source node is situated in close proximity to Γ_n, i.e. $h < h_q$
(iii) singular case, when the collocation point lies on the boundary element Γ_n.

For non-singular integration of category (i), integrals (20a–c) may be evaluated using standard Gaussian quadrature formulae if the global co-ordinates are transformed to the intrinsic co-ordinates.

Turning next to category (ii), when the distance h between the source point ξ and the boundary element Γ_n is less than the specified quasi-singular distance h_q, we should utilize higher-order Gaussian quadrature to accurately capture the kernel behaviour. In order to increase the numerical integration efficiency, a non-linear transformation similar to that proposed by Telles[20] is used.

Particular emphasis should be placed on the accurate determination of category (iii) integrals when integrands u^*_{ik} and t^*_{ik} exhibit singularity at $x \to \xi^{(m)}$. As will readily be observed, the free space Green function u^*_{ik} introduces an ln r-type singularity and integral (20b) is integrable at every N_α, $\alpha = 1, 2, 3$, while the traction tensor t^*_{ik} has a $1/r$-type singularity and thus (20a) is integrable only for specific combinations of α and the source node location on the boundary element. In the case where α coincides with the local number of the node, integral (20a) exists only in the Cauchy principal value sense and cannot be evaluated directly.

To analytically integrate (20b), consider the boundary element referring to the straight segment showing in Figure 1. The fundamental solution (12) may be written as

$$u^*_{ik}(V, y) = \delta_{ik} \tilde{h}^*(v) + h^*_{ik}(v) - h^*_{ik}(\mu), \tag{21}$$

where

$$\tilde{h}^*(v) = \frac{1}{2\pi v} \exp\left(-\frac{y_j V_j}{2v}\right) K_0\left(\frac{rV}{2v}\right) \tag{22}$$

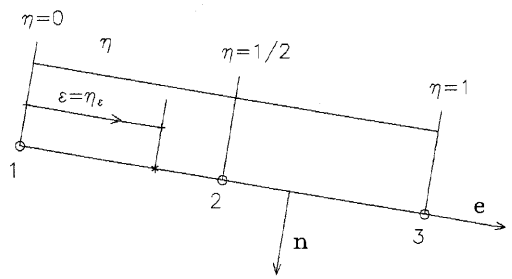

Figure 1. Boundary element integration scheme

is the fundamental solution of the convection–diffusion equation and

$$h^*_{ik}(v) = \frac{1}{4\pi v}\left\{-\delta_{ik}\exp\left(-\frac{y_j V_j}{2v}\right)K_0\left(\frac{rV}{2v}\right) + \frac{1}{rV}(V_i y_k + V_k y_i - \delta_{ik} y_j V_j)\left[\frac{2v}{rV} - \exp\left(-\frac{y_j V_j}{2v}\right)K_1\left(\frac{rV}{2v}\right)\right]\right\}. \tag{23}$$

In the case of curvilinear (quadratic) boundary elements the total integration procedure may be separated into two parts:

(i) analytical integration over the straight segment tangential to the curvilinear boundary element at the source node
(ii) numerical integration over the remaining part of the boundary element.

Part (i) is identical with the procedure outlined below if it is remembered that the integration is performed not over the whole boundary element but over its part, as provided by Shi and Banerjee.[21]

Using (21)–(23), we write integral (20b) in the form

$$H^{(\alpha)}_{ikmn} = \delta_{ik}\tilde{h}^{(\alpha)}_{mn}(v) + h^{(\alpha)}_{ikmn}(v) - h^{(\alpha)}_{ikmn}(\mu), \tag{24}$$

where

$$\tilde{h}^{(\alpha)}_{mn}(v) = L_n \int_0^1 N_\alpha(\eta)\tilde{h}^*(v)\,\mathrm{d}\eta, \tag{25a}$$

$$h^{(\alpha)}_{ikmn}(v) = L_n \int_0^1 N_\alpha(\eta)h^*_{ik}(v)\,\mathrm{d}\eta, \tag{25b}$$

$$h^{(\alpha)}_{ikmn}(\mu) = L_n \int_0^1 N_\alpha(\eta)h^*_{ik}(\mu)\,\mathrm{d}\eta. \tag{23c}$$

Considering the boundary element illustrated schematically in Figure 1, we can express the interpolating polynomials (18) as

$$N_\alpha\left(\varepsilon \pm \frac{y}{y_L}\right) = \sum_{\beta=1}^{3} a_{\alpha\beta}\left(\pm\frac{y}{y_L}\right)^{\beta-1}, \quad \alpha = 1, 2, 3,$$

in which $\varepsilon = 0$ for local node 1, $\varepsilon = \frac{1}{2}$ for node 2 and $\varepsilon = 1$ for node 3. The coefficients $a_{\alpha\beta}$ are given by

$$\mathbf{a} = \begin{bmatrix} 1 - 3\varepsilon + 2\varepsilon^2 & 4\varepsilon - 3 & 2 \\ 4\varepsilon - 4\varepsilon^2 & 4 - 8\varepsilon & -4 \\ 2\varepsilon^2 - \varepsilon & 4\varepsilon - 1 & 2 \end{bmatrix}.$$

Next we obtain integrals (25a) as

$$\tilde{h}^{(\alpha)}_{mn}(v) = \frac{1}{\pi V} \sum_{\beta=1}^{3} a_{\alpha\beta} y_L^{1-\beta} [(-1)^{\beta-1} P_{\beta-1}(\varepsilon y_L, \gamma^*) + P_{\beta-1}(y_L - y_L \varepsilon, \gamma)], \tag{26}$$

where

$$y_L = \frac{L_n V}{2v}, \qquad \gamma = e_i v_i, \qquad \gamma^* = -\gamma,$$

e_i is the vector tangent to the boundary element,

$$e_1 = -n_2, \qquad e_2 = n_1,$$

$v_i = V_i/V$ is the unit convective velocity vector and L_n is the boundary element length. The evaluation of the integral

$$P_k(y_L, \gamma) = \int_0^{y_L} y^k \exp(-\gamma y) K_0(y)\, \mathrm{d}y, \quad k = 0, 1, 2, 3, 4, \tag{27}$$

is detailed in Appendix I. Integral (25b) can be stated as

$$h^{(\alpha)}_{ikmn}(v) = -\tfrac{1}{2}\delta_{ik}\tilde{h}^{(\alpha)}_{mn}(v) + \tfrac{1}{2}[v_i Q^{(\alpha)}_k(v) + v_k Q^{(\alpha)}_i(v) - \delta_{ik} v_j Q^{(\alpha)}_j(v)], \tag{28}$$

in which the integral $Q^{(\alpha)}_i(v)$ is given by

$$Q^{(\alpha)}_i(v) = \frac{e_i}{\pi V} \sum_{\beta=1}^{3} a_{\alpha\beta} y_L^{1-\beta} [(-1)^{\beta} T_{\beta-1}(\varepsilon y_L, \gamma^*) + T_{\beta-1}(y_L - y_L \varepsilon, \gamma)]. \tag{29}$$

The analytical integration of

$$T_k(y_L, \gamma) = \int_0^{y_L} y^k \left(\frac{1}{y} - \exp(-\gamma y) K_1(y) \right) \mathrm{d}y, \quad k = 0, 1, 2, 3, 4, \tag{30}$$

is provided in Appendix II. Next we express (20a) as

$$G^{(\alpha)}_{ikmn} = \tilde{g}^{(\alpha)}_{ikmn}(v) + g^{(\alpha)}_{ikmn}(v) - g^{(\alpha)}_{ikmn}(\mu), \tag{31}$$

where

$$\tilde{g}^{(\alpha)}_{ikmn}(v) = L_n \int_0^1 N_\alpha(\eta) \tilde{g}^*_{ik}(v)\, \mathrm{d}\eta, \tag{32a}$$

$$g^{(\alpha)}_{ikmn}(v) = L_n \int_0^1 N_\alpha(\eta) g^*_{ik}(v)\, \mathrm{d}\eta, \tag{32b}$$

$$g^{(\alpha)}_{ikmn}(\mu) = L_n \int_0^1 N_\alpha(\eta) g^*_{ik}(\mu)\, \mathrm{d}\eta. \tag{32c}$$

In (32a–c) the following notation is used:

$$\tilde{g}^*_{ik}(v) = -\tfrac{1}{2}\delta_{ik}V_j n_j \tilde{h}^*(v) - \tfrac{1}{2}V_i n_k \tilde{h}^*(v) - \delta_{ik}\frac{V}{2\pi v}\frac{y_j n_j}{2r}\exp\left(-\frac{y_j V_j}{2v}\right)K_1\left(\frac{rV}{2v}\right)$$
$$-\frac{V}{2\pi v}\frac{y_i n_k}{2r}\exp\left(-\frac{y_j V_j}{2v}\right)K_1\left(\frac{rV}{2v}\right) - \frac{\lambda}{2v}V_k n_i \tilde{h}^*(v) - \frac{\lambda V}{2\pi v^2}\frac{y_k n_i}{2r}\exp\left(-\frac{y_j V_j}{2v}\right)K_1\left(\frac{rV}{2v}\right), \quad (33)$$

$$g^*_{ik}(\tilde{\mu}) = \frac{v}{4\pi\tilde{\mu}}\left\{(\delta_{ik}v_j n_j - n_k v_i)\frac{V}{2\tilde{\mu}}\exp\left(-\frac{y_j V_j}{2\tilde{\mu}}\right)K_0\left(\frac{rV}{2\tilde{\mu}}\right) + (\delta_{ik}y_j n_j + n_k y_i)\frac{V}{2\tilde{\mu}r}\exp\left(-\frac{y_j V_j}{2\tilde{\mu}}\right)K_1\left(\frac{rV}{2\tilde{\mu}}\right)\right.$$
$$-\frac{2}{r^3}[y_j n_j(y_k v_i + y_i v_k - \delta_{ik}y_j v_j) + y_i(y_k v_j n_j + v_k y_j n_j - n_k y_j v_j)]\left[\frac{2\tilde{\mu}}{rV} - \exp\left(-\frac{y_j V_j}{2\tilde{\mu}}\right)K_1\left(\frac{rV}{2\tilde{\mu}}\right)\right]$$
$$+\frac{2n_i v_k}{r}\left[\frac{2\tilde{\mu}}{rV} - \exp\left(-\frac{y_j V_j}{2\tilde{\mu}}\right)K_1\left(\frac{rV}{2\tilde{\mu}}\right)\right]$$
$$+\frac{V}{2\tilde{\mu}r^2}[y_j n_j(y_k v_i + y_i v_k - \delta_{ik}y_j v_j) + y_i(y_k v_j n_j + v_k y_j n_j - n_k y_j v_j)]\exp\left(-\frac{y_j V_j}{2\tilde{\mu}}\right)K_0\left(\frac{rV}{2\tilde{\mu}}\right)$$
$$\left.+\frac{V}{2\tilde{\mu}r}[v_j n_j(y_k v_i + y_i v_k - \delta_{ik}y_j v_j) + v_i(y_k v_j n_j + v_k y_j n_j - n_k y_j v_j)]\exp\left(-\frac{y_j V_j}{2\tilde{\mu}}\right)K_1\left(\frac{rV}{2\tilde{\mu}}\right)\right\}$$
$$+\frac{\lambda V n_i}{4\pi\tilde{\mu}^2}\left[v_k\exp\left(-\frac{y_j V_j}{2\tilde{\mu}}\right)K_0\left(\frac{rV}{2\tilde{\mu}}\right) + \frac{y_k}{r}\exp\left(-\frac{y_j V_j}{2\tilde{\mu}}\right)K_1\left(\frac{rV}{2\tilde{\mu}}\right)\right], \quad (34)$$

where $\tilde{\mu}$ is equal to v and μ for (32b,c) respectively. Substituting (33) into (32a) and using the identity $y_j n_j = 0$, we obtain

$$\tilde{g}^{(\alpha)}_{ikmn}(v) = -\frac{V}{2}\left[\left(\delta_{ik}v_j n_j + v_i n_k + \frac{\lambda}{v}v_k n_i\right)\tilde{h}^{(\alpha)}_{mn}(v) + \left(n_k R^{(\alpha)}_i(v) + \frac{\lambda}{v}n_i R^{(\alpha)}_k(v)\right)\right], \quad (35)$$

where

$$R^{(\alpha)}_i(v) = -Q^{(\alpha)}_i(v) + \tilde{R}^{(\alpha)}_i, \quad (36)$$

$$\tilde{R}^{(\alpha)}_i = \frac{L_n}{\pi V}\int_0^1 \frac{y_i}{r}N_\alpha(\eta)\,\mathrm{d}\eta. \quad (37)$$

Evidently, if the local nodal point number coincides with α, integrals (32) cannot be evaluated owing to a $1/\eta$-type singularity in the integrands. Otherwise, the integrals contain solely a weak singularity. Thus we can present integral (37) in the form

$$\alpha = 1: \quad \tilde{R}^{(1)}_i = \frac{2e_i}{\pi V}(\varepsilon - 1) \quad \text{for } \varepsilon \neq 0, \quad (38a)$$

$$\alpha = 2: \quad \tilde{R}^{(2)}_i = \frac{2e_i}{\pi V}(1 - 2\varepsilon) \quad \text{for } \varepsilon \neq \tfrac{1}{2}, \quad (38b)$$

$$\alpha = 3: \quad \tilde{R}^{(3)}_i = \frac{2e_i}{\pi V}\varepsilon \quad \text{for } \varepsilon \neq 1. \quad (38c)$$

Let us next express integrals (32b,c) as

$$g^{(\alpha)}_{ikmn}(\tilde{\mu}) = \frac{V}{2\tilde{\mu}}\left(\lambda n_i v_k + \frac{v}{2}(\delta_{ik} v_j n_j + n_k v_i)\right)\tilde{h}^{(\alpha)}_{mn}(\tilde{\mu}) + \frac{V}{2\tilde{\mu}}\left(\lambda n_i + \frac{v}{2} v_j n_j v_i\right) R^{(\alpha)}_k(\tilde{\mu})$$
$$+ \frac{v}{4\tilde{\mu}}[V(n_k + v_j n_j v_k) R^{(\alpha)}_i(\tilde{\mu}) - 4\tilde{\mu} v_j n_j Y^{(\alpha)}_{ik}(\tilde{\mu}) + 4\tilde{\mu} n_k v_j Y^{(\alpha)}_{ij}(\tilde{\mu}) + 4\tilde{\mu} n_i v_k S^{(\alpha)}(\tilde{\mu})$$
$$+ V v_j n_j Z^{(\alpha)}_{ik}(\tilde{\mu}) - V n_k v_j Z^{(\alpha)}_{ij}(\tilde{\mu}) - \delta_{ik} V n_j v_j v_l R^{(\alpha)}_l(\tilde{\mu}) + V v_j n_j v_i R^{(\alpha)}_k(\tilde{\mu}) - V v_i n_k v_j R^{(\alpha)}_{kj}(\tilde{\mu})], \quad (39)$$

where

$$S^{(\alpha)}(\tilde{\mu}) = \frac{L_n}{2\pi\tilde{\mu}} \int_0^1 \frac{1}{r} N_\alpha(\eta)\left[\frac{2\tilde{\mu}}{rV} - \exp\left(-\frac{y_j V_j}{2\tilde{\mu}}\right) K_1\left(\frac{rV}{2\tilde{\mu}}\right)\right] \mathrm{d}\eta, \quad (40a)$$

$$Y^{(\alpha)}_{ik}(\tilde{\mu}) = \frac{L_n}{2\pi\tilde{\mu}} \int_0^1 \frac{y_i y_k}{r^3} N_\alpha(\eta)\left[\frac{2\tilde{\mu}}{rV} - \exp\left(-\frac{y_j V_j}{2\tilde{\mu}}\right) K_1\left(\frac{rV}{2\tilde{\mu}}\right)\right] \mathrm{d}\eta, \quad (40b)$$

$$Z^{(\alpha)}_{ik}(\tilde{\mu}) = \frac{L_n}{2\pi\tilde{\mu}} \int_0^1 \frac{y_i y_k}{r^3} N_\alpha(\eta) \exp\left(-\frac{y_j V_j}{2\tilde{\mu}}\right) K_0\left(\frac{rV}{2\tilde{\mu}}\right) \mathrm{d}\eta \quad (40c)$$

are given by

$$S^{(\alpha)}(\tilde{\mu}) = \frac{1}{2\pi\tilde{\mu}} \sum_{\beta=2}^{3} a_{\alpha\beta} y_L^{1-\beta}[(-1)^{\beta-1} T_{\beta-2}(\varepsilon y_L, \gamma^*) + T_{\beta-2}(y_L - \varepsilon y_L, \gamma)],$$
$$Y^{(\alpha)}_{ik}(\tilde{\mu}) = e_i e_k S^{(\alpha)}(\tilde{\mu}), \qquad Z^{(\alpha)}_{ik}(\tilde{\mu}) = e_i e_k \tilde{h}^{(\alpha)}(\tilde{\mu}).$$

Integrals (32) involve a strong $1/\eta$-type singularity and exist only in the Cauchy principal value sense if the $a_{\alpha 1}$-values are equal to unity. In the present work these integrals are evaluated indirectly using the discrete boundary integral equation (19) and uniform velocity fields (a) $u_1 = 1, u_2 = 0$ and (b) $u_1 = 0, u_2 = 1$ satisfying both the continuity and momentum equations. Here we derive the simplified representation of the integral equation (19) as

$$c_{ik}(\xi^{(m)}) + \sum_{n=1}^{4} \sum_{\alpha=1}^{3} G^{(\alpha)}_{ikmn} + \sum_{n=1}^{4} \sum_{\alpha=1}^{3} \sum_{j=1}^{2} V_j n_j H^{(\alpha)}_{ikmn} = 0, \quad (41)$$

which may be written $8d^2$ times for every volume cell, where '8' implies the number of collocation points in the cell and $d = 2$ is the dimensionality of the problem. It is obvious that there are also $8d^2$ strongly singular coefficients $G^{(\alpha)}_{ikmn}$ and, in consequence, their values can be calculated from the discrete integral equation (41) if c_{ik} and $G^{(\alpha)}_{ikmn}$ are previously combined. Ultimately, the values of $c_{ik}(\xi^{(m)})$ need not be obtained in an explicit form.

Next we represent integral (20c) containing the product of functions $N_\alpha(\eta)$ and $N_\beta(\eta)$ as

$$\tilde{F}^{(\alpha,\beta)}_{ikmn} = \delta_{ik} \tilde{f}^{(\alpha,\beta)}_{mn}(v) + f^{(\alpha,\beta)}_{ikmn}(v) - f^{(\alpha,\beta)}_{ikmn}(\mu), \quad (42)$$

where

$$\tilde{f}^{(\alpha,\beta)}_{mn}(v) = L_n \int_0^1 N_\alpha(\eta) N_\beta(\eta) \tilde{h}^*(v) \, \mathrm{d}\eta, \quad (43a)$$

$$f^{(\alpha,\beta)}_{ikmn}(v) = L_n \int_0^1 N_\alpha(\eta) N_\beta(\eta) h^*_{ik}(v) \, \mathrm{d}\eta, \quad (43b)$$

$$f^{(\alpha,\beta)}_{ikmn}(\mu) = L_n \int_0^1 N_\alpha(\eta) N_\beta(\eta) h^*_{ik}(\mu) \, \mathrm{d}\eta. \quad (43c)$$

Substituting the interpolating polynomials $N_\alpha(\eta)$ and expression (22) into (43a), we obtain

$$\begin{aligned}\tilde{f}_{mn}^{(\alpha,\beta)}(v) = &\frac{1}{\pi V}\{a_{\alpha1}a_{\beta1}[P_0(\varepsilon y_L,\gamma^*)+P_0(y_L-\varepsilon y_L,\gamma)]\\ &+(a_{\alpha1}a_{\beta2}+a_{\alpha2}a_{\beta1})[-P_1(\varepsilon y_L,\gamma^*)+P_1(y_L-\varepsilon y_L,\gamma)]/y_L\\ &+(a_{\alpha1}a_{\beta3}+a_{\alpha2}a_{\beta2}+a_{\alpha3}a_{\beta1})[P_2(\varepsilon y_L,\gamma^*)+P_2(y_L-\varepsilon y_L,\gamma)]/y_L^2\\ &+(a_{\alpha2}a_{\beta3}+a_{\alpha3}a_{\beta2})[-P_3(\varepsilon y_L,\gamma^*)+P_3(y_L-\varepsilon y_L,\gamma)]/y_L^3\\ &+a_{\alpha3}a_{\beta3}[P_4(\varepsilon y_L,\gamma^*)+P_4(y_L-\varepsilon y_L,\gamma)]/y_L^4\}.\end{aligned}$$

Integral (43b) may be written as

$$f_{ikmn}^{(\alpha,\beta)}(v) = -\frac{\delta_{ik}}{2}\tilde{f}_{mn}^{(\alpha,\beta)}(v)+\frac{1}{2V}[V_i\tilde{q}_k^{(\alpha,\beta)}(v)+V_k\tilde{q}_i^{(\alpha,\beta)}(v)-\delta_{ik}V_j\tilde{q}_j^{(\alpha,\beta)}(v)], \tag{44}$$

where $\tilde{q}_i^{(\alpha,\beta)}(v)$ is given by

$$\begin{aligned}\tilde{q}_i^{(\alpha,\beta)}(v) = &\frac{e_i}{\pi V}\{a_{\alpha1}a_{\beta1}[-T_0(\varepsilon y_L,\gamma^*)+T_0(y_L-\varepsilon y_L,\gamma)]\\ &+(a_{\alpha1}a_{\beta2}+a_{\alpha2}a_{\beta1})[T_1(\varepsilon y_L,\gamma^*)+T_1(y_L-\varepsilon y_L,\gamma)]/y_L\\ &+(a_{\alpha1}a_{\beta3}+a_{\alpha2}a_{\beta2}+a_{\alpha3}a_{\beta1})[-T_2(\varepsilon y_L,\gamma^*)+T_2(y_L-\varepsilon y_L,\gamma)]/y_L^2\\ &+(a_{\alpha2}a_{\beta3}+a_{\alpha3}a_{\beta2})[T_3(\varepsilon y_L,\gamma^*)+T_3(y_L-\varepsilon y_L,\gamma)]/y_L^3\\ &+a_{\alpha3}a_{\beta3}[-T_4(\varepsilon y_L,\gamma^*)+T_4(y_L-\varepsilon y_L,\gamma)]/y_L^4\}.\end{aligned}$$

Numerical evaluation of the volume integral (20d) involves some difficulties due to the $1/\eta$-type kernel singularity. To reduce the singularity order of the integrand, we apply the divergence theorem to (20d):

$$\tilde{V}_{ijkm}^{(\alpha,\beta)} = \oint_\Gamma M_\alpha(\eta_1,\eta_2)M_\beta(\eta_1,\eta_2)u_{ik}^*(V,y)n_j(x)\,\mathrm{d}\Gamma(x)-\int_\Omega u_{ik}^*(V,y)\frac{\partial M_\alpha(\eta_1,\eta_2)M_\beta(\eta_1,\eta_2)}{\partial x_j}\mathrm{d}\Omega(x). \tag{45}$$

In that case the integrand singularity reduces to the order of $\ln r$ and thus the volume integral on the right-hand side of (45) can be evaluated accurately using a lower order of Gaussian quadrature than that of the case where the Gaussian quadrature is directly applied to (20d).

As a result of the singular nature of the kernel u_{ik}^*, every volume cell needs to be subdivided into either four or six non-overlapping triangles so that the collocation node $\xi^{(m)}$ is one of the apexes. To ensure the higher-order accuracy of volume integration at high Reynolds numbers, each triangle is additionally subdivided into several non-uniform subsegments (see Figure 2).

In order to evaluate the surface integral over Γ on the right-hand side of (45), we express it as the sum

$$\int_\Gamma M_\alpha(\eta_1,\eta_2)M_\beta(\eta_1,\eta_2)u_{ik}^*(V,y)n_j(x)\,\mathrm{d}\Gamma(x)=\sum_{n=1}^{4}n_j^{(n)}\int_{\Gamma_n}M_\alpha(\eta_1,\eta_2)M_\beta(\eta_1,\eta_2)u_{ik}^*(V,y)\,\mathrm{d}\Gamma(x). \tag{46}$$

The interpolating function $M_\alpha(\eta_1,\eta_2)$ on the contour Γ either reduces to the interpolating functions over boundary elements or is virtually nil. Accordingly, integrals over Γ_n on the right-hand side of (46) convert to the integrals $\tilde{F}_{ikmn}^{(\alpha,\beta)}$.

It is well known that the accuracy of boundary element methods essentially depends on the accuracy of evaluation of discrete integral equation coefficients and therefore it is crucial to be aware

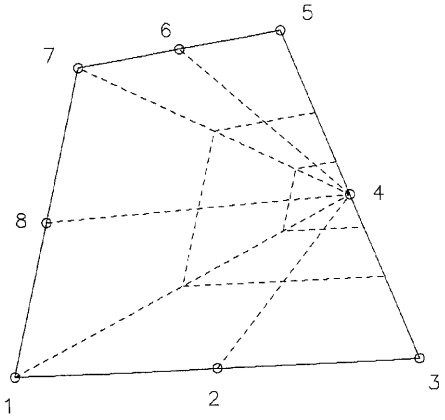

Figure 2. Volume cell subdivided into several subdomains

of the validity of their calculation. In this paper, to verify the accuracy of this step, we suggest applying the velocity field

$$u_1 = 4x_2(1 - x_2), \qquad u_2 = 0, \tag{47}$$

which is the exact solution of the Navier–Stokes equation for fully developed viscous flow between two plates. It is evident that profile (47) is appropriate for verification solely in the case of incompressible flow, i.e. $1/\lambda = 0$. The discrepancy between the left-hand and right-hand sides of (19) indicates the accuracy order in obtaining the discrete integral equation coefficients.

4.2. Numerical solution

We adopt collocation nodes at every cell node and write the discrete integral equation for each of them. Obviously, this procedure can be carried out for every cell Ω_n. It is well to bear in mind that four linearly independent discrete integral equations (two for each of neighbouring cells) may be formulated for each internal even-numbered node as well as that the number of unknowns at this node is equal to eight. Using compatibility conditions between neighbouring cells I and II, i.e.

$$u_i^{(\mathrm{I})} = u_i^{(\mathrm{II})}, \qquad t_i^{(\mathrm{I})} = -t_i^{(\mathrm{II})},$$

we reduce the number of unknowns to the number of discrete integral equations, namely four. The situation is more complicated if an odd-numbered node is considered, which, of course, is assumed to be a vertex of the cell. If the surface force t_i is considered for each of r boundary elements radiating from the star-type node, we have to utilize $2(r + 1)$ unknowns for that node. This leads to a dramatic increase in the number of global unknowns and hence the stresses σ_{ij} are used as the nodal variables in this paper. Since the tensor σ_{ij} is symmetric, we may take into consideration only three components of the tensor. Owing to this, there are only five nodal variables at the internal cell vertex, namely two velocity variables and three unknowns of the stress, whereby the tractions t_i may readily be evaluated as

$$t_i = \sigma_{i1}n_1 + \sigma_{i2}n_2.$$

This approach has also been utilized for the star-type boundary nodes lying on the smooth boundary. As for boundary corner nodes, we have not considered them as star-type nodes but simply imposed there velocities or tractions, although we should have handled these corner nodes as double nodes to

increase the accuracy of the numerical method. As will be seen in the next section, this results in poor resolution at the corners when modelling driven cavity flow.

To solve the boundary value problem, proper natural boundary conditions associated with this formulation must be specified: $\bar{u}_i$ on Γ_i and, if $\Gamma \neq \Gamma_1$ (and only if), we specify $\bar{t}_i$, on Γ_2. For the driven cavity problem considered in this paper, $\Gamma = \Gamma_1$ and $\Gamma_2 = \oslash$ so only the velocities must be specified on the complete boundary Γ. For other flows such as channel flows or external flows the boundary conditions will not be discussed here, although we believe that there will not be radical difficulties in such types of flows.

Once the required number of linearly independent integral equations (19) has been written and the boundary conditions specified have been exploited, we derive a global set of non-linear algebraic equations

$$\mathbf{A}(\mathbf{x})\mathbf{x} = \mathbf{b}, \tag{48}$$

where $\mathbf{x}$ is the vector of unknowns containing a mixture of generalized velocities and stresses. Since the elements of the global matrix $\mathbf{A}$ depend on the averaged convective velocity V_i which is to be refined during the iteration process, system (48) should be linearized on the assumption that the velocity V_i does not depend on $\mathbf{x}$ during an iteration step. Examining the domain discretized into a plethora of cells, we derive the banded global matrix $\mathbf{A}$ in a similar way as for finite element methods. However, the matrix is unsymmetric. In order to solve the set of equations (48), a direct iteration procedure is used here and, in doing so, the set of linear equations

$$\mathbf{A}(\mathbf{x}^{(q-1)})\mathbf{x}^{(q)} = \mathbf{b} \tag{49}$$

is solved at every iteration. In (49), q is the iteration number. To solve system (49), the direct method for solving sparse equations presented by Østerby and Zlatev[22] has been utilized in this work.

5. NUMERICAL RESULTS

The numerical algorithm proposed above has been implemented in C++ code on a personal computer, which allows us to simulate steady two-dimensional viscous fluid flows. The numerical method has been applied to square driven cavity flow, for which a large number of numerical results are available for comparison purposes. Amongst these, the most attractive is the work of Ghia *et al.*,[23] where the numerical computations were carried out using multigrid finite differences on very fine 129×129 and 257×257 grids up to $Re = 10{,}000$.

In this paper, numerical solutions for square driven cavity flow have been carried out up to $Re = 1000$ at $\lambda = 10^{10}$. The velocities on the left, bottom and right walls are fixed at zero, while unit velocity is specified on the moving top lid. The numerical examples show a very high rate of convergence. For instance, starting from the velocities equal to zero, the iteration process converges in only six steps at $Re = 100$, while nine steps are required at $Re = 400$ and 11 steps at $Re = 1000$. It is assumed that the iterations are converged when the r.m.s. flow velocity between successive iterations is less than 10^{-5} for each velocity component. The convergence rate therewith is uniform for every nodal point as evidenced by the maximum residual between successive iterations. It is notable that the iteration convergence rate has only a weak dependence on the mesh size, which can have a determining effect on the efficiency of the proposed method when using it for engineering problems with thousands of cells.

It is common knowledge that a similar high convergence rate may be achieved only if the Newton–Raphson algorithm is employed for a non-linear set of equations. Unfortunately, with the Newton–Raphson method a convergent solution may not be obtained unless the initial guess is near the true

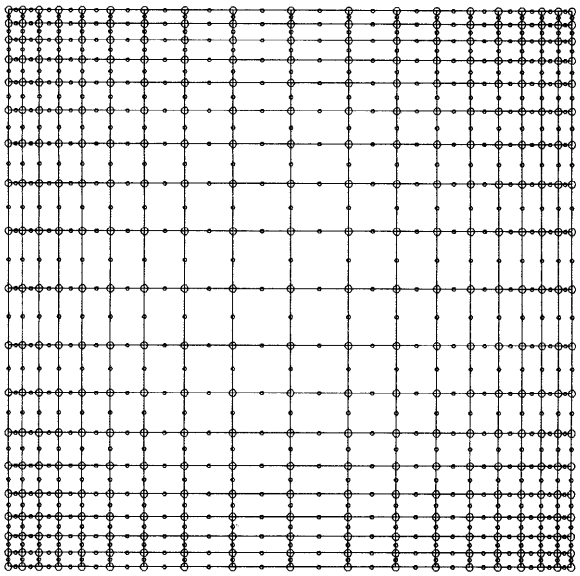

Figure 3. Boundary element model

solution. To have a good initial guess, a succession of calculations should be used at different (increasing) Reynolds numbers. It is axiomatic that this increases the computational expense.

Results are presented for a non-uniform mesh with $N_c = 324$ cells as shown in Figure 3. Figure 4 illustrates the spatial plots of the resulting velocity vectors for different Reynolds numbers. The vector plots are very similar to those obtained previously by other authors and widely covered in the literature. The numerical results are examined more comprehensively in Figure 5, where the horizontal velocities on the vertical centreline (Figure 5(a)) and the vertical velocities on the horizontal centreline (Figure 5(b)) are presented. As may be inferred from the graphs, the numerical solutions are in good agreement with those obtained by Ghia *et al.*[23]

Several properties of the primary vortices are given in Table I. The results of the present study are in good agreement with those of Ghia *et al.*[23] Unfortunately, secondary vortices were not resolved in this study owing to the poor resolution in the corner regions. To increase the accuracy of the method, we should use a finer mesh than that used here as well as handle corners as double nodes.

In this paper no numerical results are presented beyond a Reynolds number of 1000, since a more refined mesh than that used here must be employed to obtain valid results. Such calculations may be carried out either on a more powerful computer or on this personal computer if the number of global unknowns is dramatically decreased via an elimination of stresses at internal nodes from global unknowns.

Table I. Properties of primary vortices inside square driven cavity

Property	Case	$Re = 100$	$Re = 400$	$Re = 1000$
Ψ_{min}	Present study	−0.10208	−0.11164	−0.11411
	Ghia *et al.*[23]	−0.103423	−0.113909	−0.117929
Location x, y	Present study	0.610, 0.730	0.555, 0.610	0.545, 0.575
	Ghia *et al.*[23]	0.6172, 0.7344	0.5547, 0.6055	0.5313, 0.5625

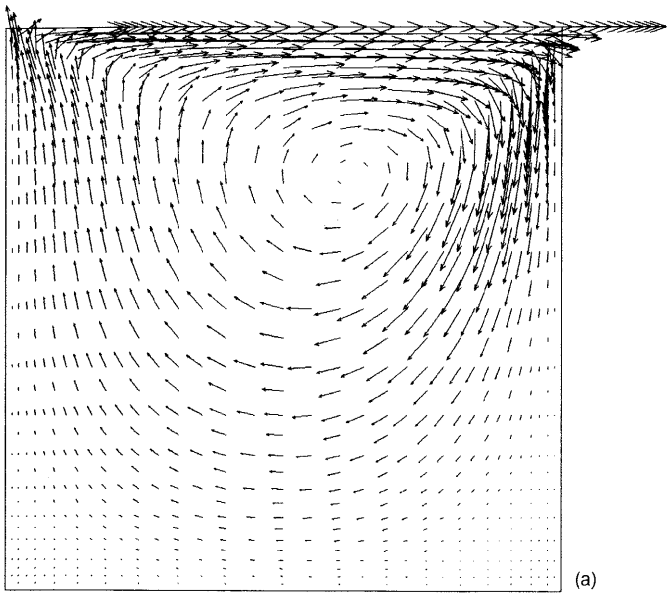

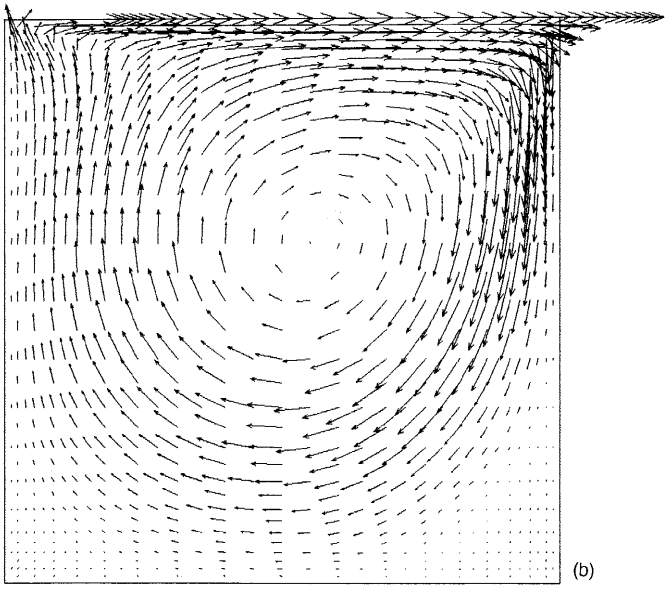

Figure 4. Velocity vectors for square driven cavity flow: (a) $Re = 100$; (b) $Re = 400$; (c) $Re = 1000$

6. CONCLUSIONS

In this paper a new boundary element method has been presented for steady two-dimensional viscous fluid flow. The numerical method is stable and exhibits a high convergence rate even when using simple iterations. It is quite apparent that these features are due to the special nature of fundamental solutions incorporating the physics of convective flow. Although the BEM technique does not permit

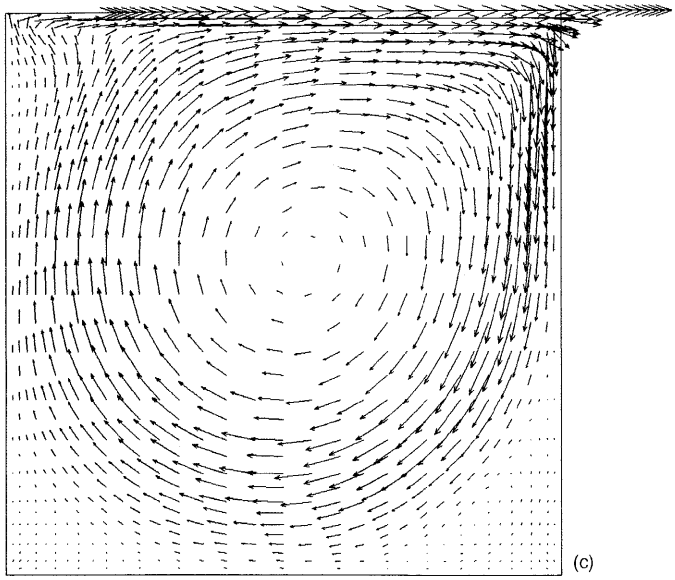

Figure 4. (*continued*)

one to reduce the problem to only a boundary problem, the efficiency of the method compares favourably with the efficiency of the most sophisticated finite element methods. This method efficiency may essentially be improved while reducing the number of nodal unknowns to two at each internal node. It should be emphasized that the proposed boundary element method enables one to model flows within very complex boundaries in a straightforward manner. From the aforesaid it might be assumed that this is a general-purpose computational method for fluid dynamics.

ACKNOWLEDGEMENTS

The authors are indebted to Dr. G. F. Dargush, State University of New York at Buffalo, for his encouragement and for giving access to his recent work.

The first author would like to acknowledge the financial support of the Russian Fund of Basic Research (grant 96-02-16751-a).

APPENDIX I: DERIVATION OF INTEGRALS P_k

The integral $P_k(y_L, \beta)$ is given by

$$P_k(y_L, \beta) = \int_0^{y_L} y^k \exp(-\beta y) K_0(y)\, \mathrm{d}y, \quad k = 0, 1, 2, 3, 4. \tag{50}$$

To integrate (50), we present the modified Bessel function of zeroth order as[24]

$$K_0(y) = -\ln\left(\frac{y}{2}\right) \sum_{n=0}^{\infty} a_n y^{2n} + \sum_{n=0}^{\infty} b_n y^{2n}, \quad 0 < y \leqslant 2, \tag{51}$$

$$K_0(y) = \frac{\exp(-y)}{\sqrt{y}} \sum_{n=0}^{6} c_n \left(\frac{2}{y}\right)^n + \varepsilon_1, \quad y > 2, \tag{52}$$

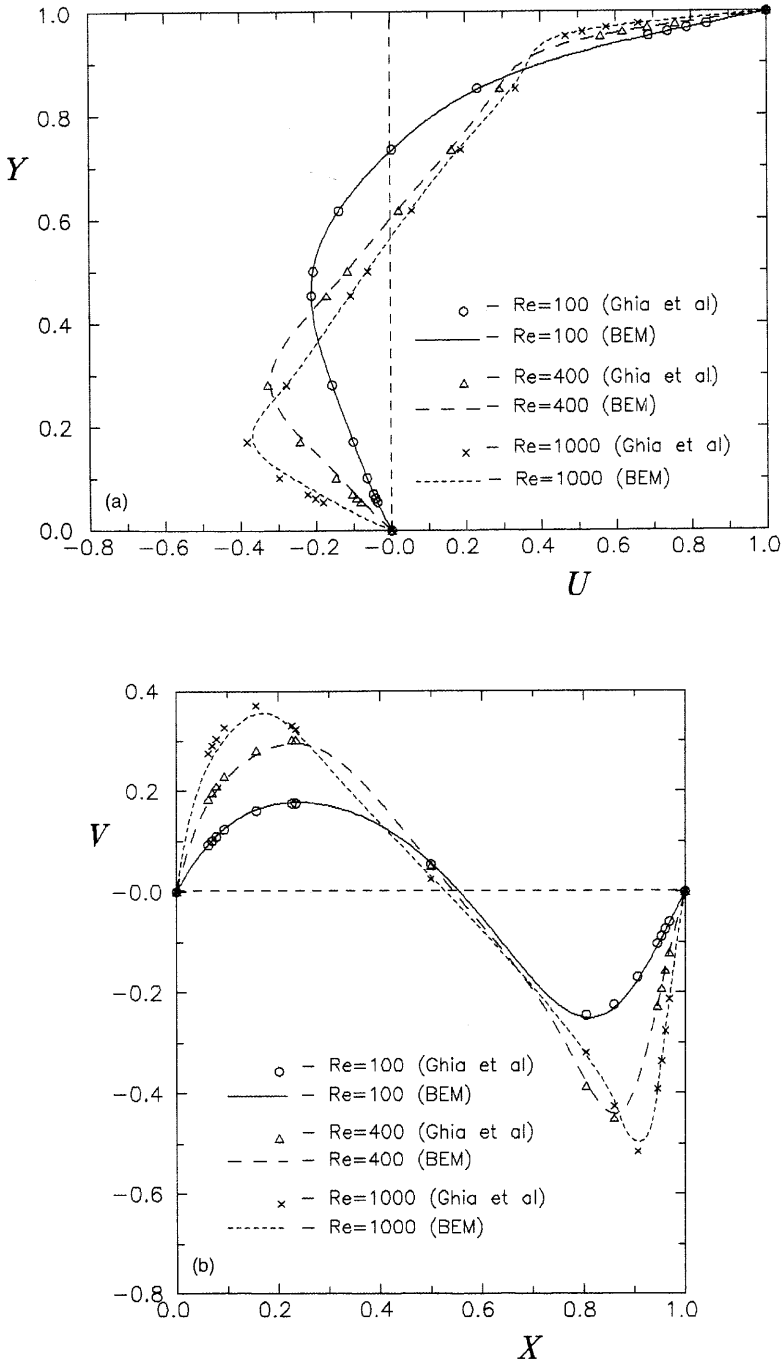

Figure 5. Velocity profiles: (a) u_1 on vertical centreline; (b) u_2 on horizontal centreline

where

$$a_n = \frac{1}{2^{2n}(n!)^2}, \quad n \geqslant 0, \qquad b_0 = -\gamma,$$

$$y \approx -0{\cdot}5772156649 \quad \text{(Euler's constant)}, \qquad b_n = a_n\left(\sum_{m=1}^{n} \frac{1}{m} - \gamma\right), \quad n \geqslant 1,$$

$$c_0 = 1{\cdot}25331414, \quad c_1 = -0{\cdot}07832358, \quad c_2 = 0{\cdot}02189568, \quad c_3 = -0{\cdot}01062446,$$

$$c_4 = 0{\cdot}00587872, \quad c_5 = -0{\cdot}00251540, \quad c_6 = 0{\cdot}00053208, \quad |\varepsilon_1| < 1{\cdot}9 \times 10^{-7}.$$

The necessity of representing $K_0(y)$ as (52) stems from the fact that series (51) is slowly convergent for large y.

Substituting (51) into (50), we derive for $y_L \leqslant 2$

$$P_k(y_L, \beta) = -\sum_{n=0}^{\infty} a_n A_{2n+k} + \sum_{n=0}^{\infty} b_n B_{2n+k}, \tag{53}$$

where

$$A_m = \int_0^{y_L} y^m \exp(-\beta y) \ln\left(\frac{y}{2}\right) \mathrm{d}y, \tag{54}$$

$$B_m = \int_0^{y_L} y^m \exp(-\beta y)\, \mathrm{d}y \tag{55}$$

are given by

$$A_0 = \frac{1}{\beta}\left[\mathrm{Ei}(-\beta y_L) - \exp(-\beta y_L) \ln\left(\frac{y_L}{2}\right) - \ln|2\beta| - \gamma\right], \quad m = 0, \tag{56}$$

$$A_m = \frac{1}{\beta}\left[mA_{m-1} + B_{m-1} - y_L^m \exp(-\beta y_L) \ln\left(\frac{y_L}{2}\right)\right], \quad m > 0, \tag{57}$$

$$B_0 = \frac{1}{\beta}[1 - \exp(-\beta y_L)], \quad m = 0, \tag{58}$$

$$B_m = \frac{1}{\beta}[mB_{m-1} - y_L^m \exp(-\beta y_L)], \quad m > 0. \tag{59}$$

In (56),

$$\mathrm{Ei}(\pm x) = \pm \exp(\pm x) \int_0^1 \frac{\mathrm{d}t}{x \pm \ln t}, \quad x > 0,$$

is the integral exponential function.[25]

Substituting (52) into (50), we obtain for $y_L > 2$

$$P_k(y_L, \beta) = P_k(2, \beta) + \sum_{n=0}^{k-1} c_n 2^n D^*_{k-n} + \sum_{n=k}^{6} c_n 2^n D_{n-k}, \tag{60}$$

where $k = 0, 1, 2, 3, 4$ and

$$D_m^* = \int_2^{y_L} y^{m-1/2} \exp(-ay)\, \mathrm{d}y = 2[f_m(\sqrt{y_L}) - f_m(\sqrt{2})], \quad m = 0, 1, \ldots, 6, \tag{61}$$

$$D_m = \int_2^{y_L} y^{-m-1/2} \exp(-ay)\, \mathrm{d}y = q_m(y_L) - q_m(2), \quad m = 1, 2, 3, 4. \tag{62}$$

In (61), $f_m(\sqrt{z})$ is given by

$$f_m(\sqrt{z}) = \frac{\exp(-az)}{(2m-1)!!2a} \sum_{j=1}^{m} (-2)^j (2m-2j-1)!! a^j z^{j-m-1/2} - \frac{(-2)^{m-1}\sqrt{\pi} a^{m-1/2}}{(2m-1)!!} \operatorname{erf}(\sqrt{(az)}), \tag{63}$$

where $\alpha = 1 + \beta$ and

$$\operatorname{erf}(z) = \frac{2}{\sqrt{\pi}} \int_0^z \exp(-t^2)\, \mathrm{d}t$$

is the error function.[25] The function $q_m(z)$ in (62) may be written as

$$q_m(z) = (2m-1)!!\sqrt{\pi} 2^{-m} a^{-m-1/2} \operatorname{erf}(\sqrt{(az)}) - \frac{1}{a} z^{m-1/2} \exp(-az) \sum_{j=0}^{m-1} \frac{(2m-1)!!}{(2m-2j-1)!!} (2az)^{-j}. \tag{64}$$

Note that (63) and (64) are inappropriate for $\beta = -1$, so in this case (61) and (62) are given by

$$D_m^* = \frac{2}{1+2m} (y_L^{m+1/2} - 2^{m+1/2}), \tag{65}$$

$$D_m = \frac{2}{1-2m} (y_L^{-m+1/2} - 2^{-m+1/2}). \tag{66}$$

As may be seen, values of A_m and B_m cannot be evaluated directly from (56)–(59) for $\beta = 0$. We obtain from (50) for $\beta = 0$ (see Reference 26 for details)

$$P_0(y_L, 0) = y_L K_0(y_L) + \tfrac{1}{2}\pi y_L [L_0(y_L) K_1(y_L) + L_1(y_L) K_0(y_L)], \tag{67}$$

in which $L_0(.)$ and $L_1(.)$ are modified Struve functions,[24] and

$$P_1(y_L, 0) = 1 - y_L K_1(y_L), \tag{68}$$

$$P_2(y_L, 0) = -y_L^2 K_1(y_L) + \tfrac{1}{2}\pi y_L [L_0(y_L) K_1(y_L) + L_1(y_L) K_0(y_L)], \tag{69}$$

$$P_3(y_L, 0) = -y_L (y_L^2 + 4) K_1(y_L) - 2y_L^2 K_0(y_L) + 4. \tag{70}$$

The value of $P_4(y_L, 0)$ may be obtained using standard Gaussian quadrature, as the integrand does not involve any singularity for $k = 4$.

APPENDIX II: DERIVATION OF INTEGRALS T_k

To obtain the integral

$$T_k(y_L, \beta) = \int_0^{y_L} y^k \left(\frac{1}{y} - \exp(-\beta y) K_1(y) \right) \mathrm{d}y, \quad k = 0, 1, 2, 3, 4, \tag{71}$$

the modified Bessel function of the second kind of first order is represented by

$$K_1(y) = \frac{1}{y} + \ln\left(\frac{y}{2}\right) \sum_{n=0}^{\infty} p_n y^{2n+1} - \sum_{n=0}^{\infty} q_n y^{2n+1}, \quad 0 < y \leqslant 2, \tag{72}$$

$$K_1(y) = \frac{\exp(-y)}{\sqrt{y}} \sum_{n=0}^{6} s_n \left(\frac{2}{y}\right)^n + \varepsilon_2, \quad y > 2, \tag{73}$$

where

$$p_n = \frac{1}{2^{2n+1} n!(n+1)!}, \quad n \geqslant 0,$$

$$q_n = \left(-\gamma + \sum_{k=1}^{n} \frac{1}{k} + \frac{1}{2(n+1)}\right) p_n, \quad n \geqslant 0,$$

$$s_0 = 1{\cdot}25331414, \quad s_1 = 0{\cdot}23498619, \quad s_2 = -0{\cdot}03655620, \quad s_3 = 0{\cdot}01504268,$$

$$s_4 = -0{\cdot}00780353, \quad s_5 = 0{\cdot}00325614, \quad s_6 = -0{\cdot}00068245, \quad |\varepsilon_2| < 2{\cdot}2 \times 10^{-7}.$$

Integrating (71) for $y_L \leqslant 2$, we obtain

$$T_k(y_L, \beta) = T_k^* - \sum_{n=0}^{\infty} p_n A_{2n+k+1} + \sum_{n=0}^{\infty} q_n B_{2n+k+1}, \tag{74}$$

where

$$T_k^* = \int_0^{y_L} y^{k-1}[1 - \exp(-\beta y)] \, \mathrm{d}y \tag{75}$$

is given by

$$T_0^* = \ln(|\beta| y_L) + \gamma - \mathrm{Ei}(-\beta y_L),$$

$$T_1^* = y_L + \frac{1}{\beta}\exp(-\beta y_L) - \frac{1}{\beta},$$

$$T_2^* = \frac{y_L^2}{2} + \left(\frac{y_L}{\beta} + \frac{1}{\beta^2}\right)\exp(-\beta y_L) - \frac{1}{\beta^2},$$

$$T_3^* = \frac{y_L^3}{3} + \left(\frac{y_L^2}{\beta} + \frac{2y_L}{\beta^2} + \frac{2}{\beta^3}\right)\exp(-\beta y_L) - \frac{2}{\beta^3},$$

$$T_4^* = \frac{y_L^4}{4} + \left(\frac{y_L^3}{\beta} + \frac{3y_L^2}{\beta^2} + \frac{6y_L}{\beta^3} + \frac{6}{\beta^4}\right)\exp(-\beta y_L) - \frac{6}{\beta^4}.$$

Substituting (73) into (71), we derive for $y_L > 2$

$$T_k(y_L, \beta) = T_k(2, \beta) + \tilde{T}_k(y_L, \beta) - \sum_{n=0}^{k-1} s_n 2^n D_{k-n}^* - \sum_{n=k}^{6} s_n 2^n D_{n-k}, \tag{76}$$

where $k = 0, 1, 2, 3, 4$ and

$$\tilde{T}_k(y_L, \beta) = \int_2^{y_L} y^{k-1} \, \mathrm{d}y \tag{77}$$

is given by

$$\tilde{T}_0(y_L, \beta) = \ln\left(\frac{y_L}{2}\right), \quad k = 0, \tag{78}$$

$$\tilde{T}_k(y_L, \beta) = \frac{1}{k}(y_L^k - 2^k), \quad k > 0. \tag{79}$$

Now we consider limiting values of $T_k(y_L, \beta)$ for $\beta = 0$:

$$T_0(y_L, 0) = -\sum_{n=0}^{\infty} p_n A^*_{2n+1} + \sum_{n=0}^{\infty} q_n B^*_{2n+1}, \quad k = 0, \tag{80}$$

where

$$B^*_m = \frac{1}{m+1} y_L^{m+1}, \quad m \geqslant 0, \qquad A^*_m = \left[\ln\left(\frac{y_L}{2}\right) - \frac{1}{m+1}\right] B^*_m, \quad m \geqslant 0.$$

The other values of $T_k(y_L, \beta)$ may be expressed as

$$T_1(y_L, 0) = y_L - \tfrac{1}{2}\pi y_L[L_0(y_L)K_1(y_L) + L_1(y_L)K_0(y_L)], \tag{81}$$

$$T_2(y_L, 0) = \frac{y_L^2}{2} + y_L^2 K_0(y_L) + 2y_L K_1(y_L) - 2, \tag{82}$$

$$T_3(y_L, 0) = \frac{y_L^3}{3} + y_L^3 K_0(y_L) + 3y_L^2 K_1(y_L) - \tfrac{3}{2}\pi y_L[K_0(y_L)L_1(y_L) + K_1(y_L)L_0(y_L)], \tag{83}$$

while $T_4(y_L, 0)$ may be evaluated via Gaussian quadrature, since the integrand involves no singularity.

REFERENCES

1. C. W. Oseen, *Neuere Methoden und Ergebnisse in der Hydrodynamik*, Akademische Verlagsgesellschaft, Leipzig, 1927.
2. N. I. Muskhelishvili, *Some Basic Problems of the Mathematical Theory of Elasticity*, Noordorf, Groningen, 1953.
3. S. G. Mikhlin, *Integral Equations and Their Applications to Certain Problems in Mechanics, Mathematical Physics and Technology*, Pergamon, Oxford, 1957.
4. O. A. Ladyzhenskaya, *The Mathematical Theory of Viscous Incompressible Flow*, Gordon and Breach, London, 1969.
5. P. K. Banerjee and R. Butterfield, *Boundary Element Methods in Engineering Science*, McGraw-Hill, London, 1981.
6. C. A. Brebbia, J. C. F. Telles and L. C. Wrobel, *Boundary Element Techniques*, Springer, Berlin, 1984.
7. C. Pozrikidis, *Boundary Integral and Singularity Methods for Linearized Viscous Flow*, Cambridge University Press, Cambridge, 1992.
8. K. Onishi, T. Kuroki and M. Tanaka, 'An application of boundary element method to incompressible laminar viscous flows', *Eng. Anal.*, **1**, 122–127 (1984).
9. P. Skerget, A. Alujevic and C. A. Brebbia, 'Vorticity–velocity–pressure boundary integral formulation', in M. Tanaka and C. A. Brebbia (eds), *Boundary Elements*, Vol. 8, *Proc. 8th Int. Conf. on BEM*, CM Publications, Southampton, 1986, Vol. 2, pp. 829–834.
10. C. V. Camp and G. S. Gipson, 'A boundary element method for viscous flows at low Reynolds numbers', *Eng. Anal. Bound. Elem.*, ***6***, 144–151 (1989).
11. J. C. Wu, 'Boundary element solution of viscous flow problems', in C. A. Brebbia (ed.), *Boundary Element Technique: Applied Fluid Flow and Computational Aspects, Proc. Int. Conf.*, Springer, Berlin, 1987, pp. 1–15.
12. M. M. Grigor'ev, 'A boundary element formulation using the SIMPLE method', *Int. j. numer. methods fluids*, **16**, 549–579 (1993).
13. N. Tosaka, K. Kakuda and K. Onishi, 'Boundary element analysis of steady viscous flows based on *P–U–V* formulation', in C. A. Brebbia and G. Maier (eds), *Boundary Elements*, Vol. 7, *Proc. 7th Int. Conf. on BEM*, CM Publications, Southampton, 1985, pp. 9/71–9/80.
14. G. F. Dargush and P. K. Banerjee, 'A boundary element method for steady incompressible thermoviscous flow', *Int. j. numer. methods eng.*, **31**, 1605–1626 (1991).
15. K. Kitagawa, L. C. Wrobel, C. A. Brebbia and M. Tanaka, 'A boundary element formulation for natural convection problems', *Int. j. numer. methods fluids*, **8**, 139–144 (1988).
16. K. Kitagawa, 'Boundary element analysis of viscous flow', in *Lecture Notes in Engineering*, Springer, Berlin, 1990.

17. K. Kakuda and N. Tosaka, 'The generalized boundary element approach for viscous fluid flow problems', *Proc. 1st Joint Japan/US Symp. on BEM*, Pergamon, Oxford, 1988, pp. 305–314.
18. M. B. Bush, 'Modelling two-dimensional flow past arbitrary cylindrical bodies using boundary element formulations', *Appl. Math. Model.*, **7**, 386–394 (1983).
19. M. M. Grigoriev, 'Fundamental solutions of Navier–Stokes equations for unsteady incompressible fluid flow using penalty function formulation', *Dok. Akad. Nauk Rossii*, **341**, 626–629 (1995) (in Russian).
20. J. C. F. Telles, 'A self-adaptive coordinate transformation for efficient numerical evaluation of general boundary element integrals', *Int. j. numer. methods eng.*, **24**, 959–973 (1987).
21. Y. Shi and P. K. Banerjee, 'Boundary element methods for convective heat transfer', *Comput. Methods Appl. Mech. Eng.*, **105**, 261–284 (1993).
22. O. Østerby and Z. Zlatev, 'Direct methods for sparse matrices', in *Lecture Notes in Computer Science*, Vol. 157, pp. 1–119, Springer, Berlin, 1983.
23. U. Ghia, K. N. Ghia and C. T. Shin, 'High-Re solutions for incompressible flow using the Navier–Stokes equations and a multigrid method', *J. Comput. Phys.*, **48**, 387–411 (1982).
24. M. Abramowitz and I. A. Stegun, *Handbook of Mathematical Functions*, Dover, New York, 1972.
25. I. S. Gradshtein and I. M. Ryzhik, *Tables of Integrals, Series and Products*, Academic, New York, 1980.
26. A. P. Prudnikov, Yu. A. Brychkov and O. I. Marichev, *Integrals and Series, Special Functions*, Nauka, Moscow, 1983 (in Russian).

